



Chemistry A European Journal

 **Chemistry
Europe**
European Chemical
Societies Publishing

Accepted Article

Title: Diazaboryl-Naphthyl-Ketone: a New Scaffold with Bright Fluorescence, Aggregation-Induced Emission, and Application in the Quantitation of Trace Boronic Acids in Pharma Intermediates

Authors: Hannah E. Hackney, Marco Paladino, Hao Fu, and Dennis G. Hall

This manuscript has been accepted after peer review and appears as an Accepted Article online prior to editing, proofing, and formal publication of the final Version of Record (VoR). This work is currently citable by using the Digital Object Identifier (DOI) given below. The VoR will be published online in Early View as soon as possible and may be different to this Accepted Article as a result of editing. Readers should obtain the VoR from the journal website shown below when it is published to ensure accuracy of information. The authors are responsible for the content of this Accepted Article.

To be cited as: *Chem. Eur. J.* 10.1002/chem.202003248

Link to VoR: <https://doi.org/10.1002/chem.202003248>

WILEY-VCH

Diazaboryl-Naphthyl-Ketone: a New Scaffold with Bright Fluorescence, Aggregation-Induced Emission, and Application in the Quantitation of Trace Boronic Acids in Pharmaceutical Intermediates

Hannah E. Hackney,^[a] Marco Paladino,^[a] Hao Fu,^[a] and Dennis G. Hall*^[a]

[a] H. Hackney, Dr. M. Paladino, H. Fu, Prof. Dr. D. G. Hall
Department of Chemistry, 4-010 CCIS
University of Alberta
Edmonton, Alberta, T6G 2G2 (Canada)
E-mail: dennis.hall@ualberta.ca

Supporting information for this article is given via a link at the end of the document.

Abstract: This study describes the synthesis, structure, and photophysical properties of a new luminescent polyaromatic boronic acid scaffold, diazaboryl-naphthyl-ketones (DNKs). These stable compounds display extremely bright fluorescence, aggregation-induced emission, positive solvatochromism, and solid state fluorescence. DFT calculations and X-ray crystallographic study revealed notable electronic and structural differences between these compounds and the parent diaminonaphthalene (DAN) adducts. Acylation of the DAN system causes a localization of both HOMO and LUMO onto the DNK unit, which supports the negligible influence of the B-aryl substituent. The LUMO energy is lowered, and its shape significantly altered. Photophysical data in solution and the solid state revealed blue-shifted, narrowed, and intense emissions for DNKs (up to 89% quantum yield). The potential utility of the fluorogenic DNK system was demonstrated with a proof-of-concept for the determination of trace boronic acid contaminants in solid samples, down to one-ppm level, using HPLC with fluorescence detection. This method could be useful in pharmaceutical development for the quantitation of difficult-to-detect and potentially mutagenic residual boronic acid from late cross-coupling reactions in drug syntheses.

Heteroatom doping is a popular strategy to modulate the electronic properties of graphene, nanographenes, and polyaromatic hydrocarbons (PAHs).¹ One area of study, beginning with the pioneering work of Dewar and coworkers in the 1960s, applies the B–N bond as a replacement for C=C bonds in aromatic structures.^{2–4} Though the two moieties are isoelectronic and isosteric, B–N replacement can significantly alter the photophysical, aromatic and electronic properties of the molecule, thereby enriching the chemical space of aromatics and diversifying their optoelectronic applications.⁵ In elaboration of this strategy, N–B–N bond patterns have the potential to offer considerable advantage. Analogous to boronic esters, the nitrogen lone pairs electronically shield the boron's vacant p orbital, substantially improving stability when compared to boronic B–N compounds.⁶ With its 4-electron count, the N–B–N unit can act as a heteroarene replacement (Figure 1A). Furthermore, it offers versatility for further functionalization, as

N–B–N rings can be inert to Suzuki-Miyaura cross-coupling conditions.⁷

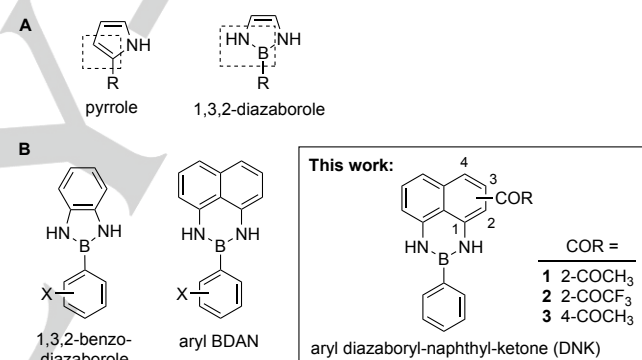


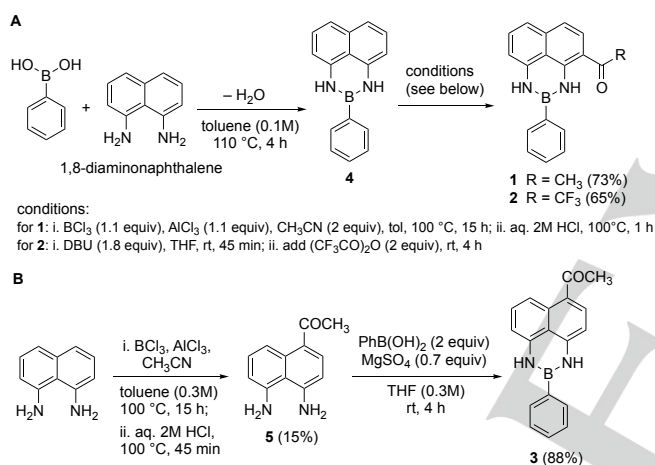
Figure 1. A. Pyrrole ring with the corresponding CC/BN isoelectronic and isosteric 1,3,2-diazaboroles, a class of N–B–N luminogens. B. 1,3,2-Benzodiazaboroles, 1,8-diaminonaphthyl boronamide (BDAN), and the generic structure of the DNK scaffold with model compounds 1–3 investigated herein.

The best-studied N–B–N motif, 1,3,2-diazaborole, represents a class of five-membered heterocycles that are isosteric with pyrroles (Figure 1A).^{8–10} In addition to their attractive properties as ligands and for electrochemistry, these compounds often exhibit extremely high luminescence quantum yields both in solution and in the solid state. A recent paper by Wan and coworkers compared 1,3,2-benzodiazaboroles with their six-membered ring counterparts, naphthodiazaborines (BDANs) (Figure 1B).¹¹ Since the pioneering work of Suginome, aryl-BDANs have become a popular class of protected arylboronic acids.⁷ However, these stable and colourless solids display very weak fluorescence in solution and as solids (QY 0.1–3%),¹¹ and consequently they remain underexplored as optoelectronic materials.

In the course of a different project, an acylation reaction on a DAN-protected arylboronic acid yielded two primary products that were intensely hued and fluoresced blue under visible light and hand-held UV lamp. This optical behaviour was dramatically different from the expected product and starting material. These

serendipitous products were characterized as the novel diazaboryl-naphthyl-ketones (DNK) of the type shown in Figure 1B. Herein we report that this simple modification of the familiar aryl-BDAN structure dramatically alters the photophysics of the scaffold, with markedly improved fluorescence quantum yields. In contrast to aryl-BDANs and 1,3,2-diazaborolines, simple structural tuning of DNKs can produce a library with a rich variety of optical properties, such as extremely bright fluorescence, aggregation-induced emission, and positive solvatochromism, which could enable new and useful applications in optoelectronics and chemical analysis.

Two unoptimized, modular strategies were employed to produce the three prototypic DNK compounds **1-3** evaluated in this study (Fig. 1B). In the first approach, Suginome's DAN condensation of phenylboronic acid is used to prepare PhBDAN **4**.⁷ The latter is then subjected to the Sugasawa reaction, a method designed to give ortho-substituted anilines regioselectively from various nitriles,¹² giving predominantly the ortho product **1** (Scheme 1A). Acylation using base and trifluoroacetic anhydride afforded DNK **2**.



Scheme 1. Synthesis of PhBDAN **4** and model DNKs **1-3** via Sugasawa reaction of: **A.** PhBDAN **4**; and, **B.** 1,8-diaminonaphthalene.

The second strategy applies the Sugasawa reaction conditions directly onto 1,8-diaminonaphthalene. However, as shown in Scheme 1B, the reaction furnishes exclusively the para-substituted DNK derivative **3**.¹³ Despite the low yield of diamine **5** in this anomalous Sugasawa reaction, it is scalable and it employs cheap reactants. The three prototypic DNKs **1-3** underwent thorough characterisation and study, beginning with structural analysis via NMR and single crystal X-ray crystallography.¹⁴

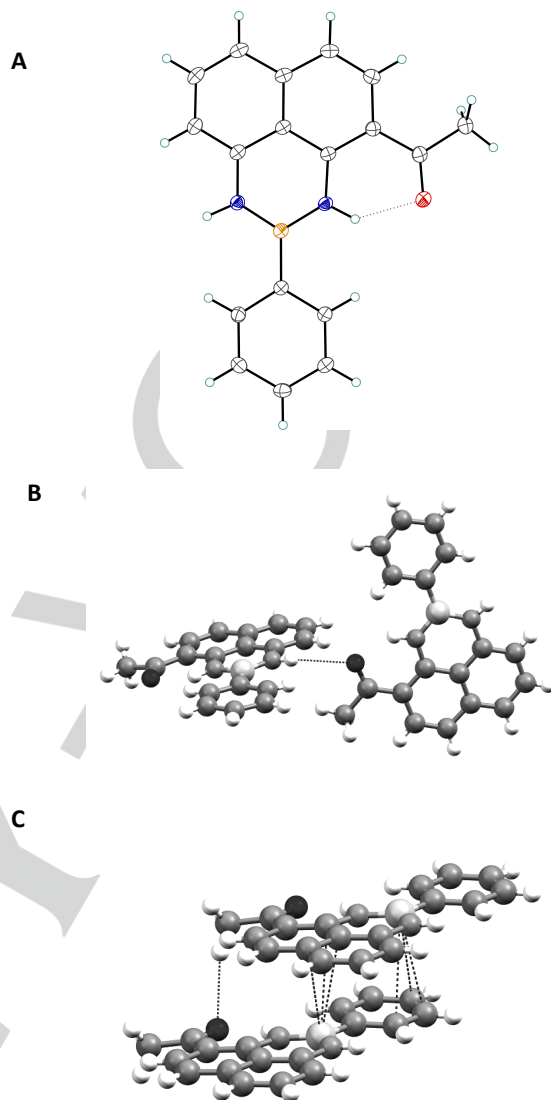


Figure 2. ORTEP drawings of DNKs **1**: **A.** Molecular representation; **B** and **C:** selected intermolecular contacts in crystal lattice.

The X-ray crystallographic structures of **1** (Figure 2) and **2**¹⁴ show that both compounds are highly planar through the diazaboryl-naphthyl rings, with the diazaboryl unit slightly twisted with respect to the B-phenyl ring.¹⁵ The short intramolecular hydrogen bond between the carbonyl oxygen and the N–H moiety (¹H NMR $\delta \sim 12$ ppm) is clearly visible in each (**1**: 1.953(15) Å, **2**: 1.77(5) Å), holding the ketone coplanar with the naphthyl substructure.¹⁴ The carbonyl of DNK **1** also exhibits a long intermolecular hydrogen bond of 2.687(1) Å with a N atom (Figure 2B), which is absent in analog **2**. Both compounds exhibit a herringbone packing mode, and the boron atom of both species also interacts with the π orbital of adjacent aryl rings (Figure 2C), potentially enriching the vacant p_z orbital. It is also instructive to contrast **1** with the published crystal structure of PhBDAN **4**.¹⁶ Specifically, **4** is also planar through the diazaboryl-naphthyl rings, however it has a markedly different packing mode dominated with T-shaped π stacking, and fewer short contacts.

Next, photophysical data was collected for DNKs **1-3**. Confirming our qualitative observations of fluorescence under UV and visible lighting conditions, the absorption and fluorescence emission spectrum of DNK **1** in acetonitrile revealed that absorptions in both wavelength ranges gave the same cyan emission at 455 nm (Figure 3A). It is noteworthy that substitution on the B-aryl ring of DNK **1** (DNKs **S6**: 4-MeOC₆H₄; **S7**: 3,4,5-F₃C₆H₂; **S8**: 2,6-Me₂C₆H₃)¹⁴ leads to very similar profiles and λ_{max} values (see S.I.), indicating that the B-phenyl ring of **1-3** does not make a significant impact on the fluorescence in solution.

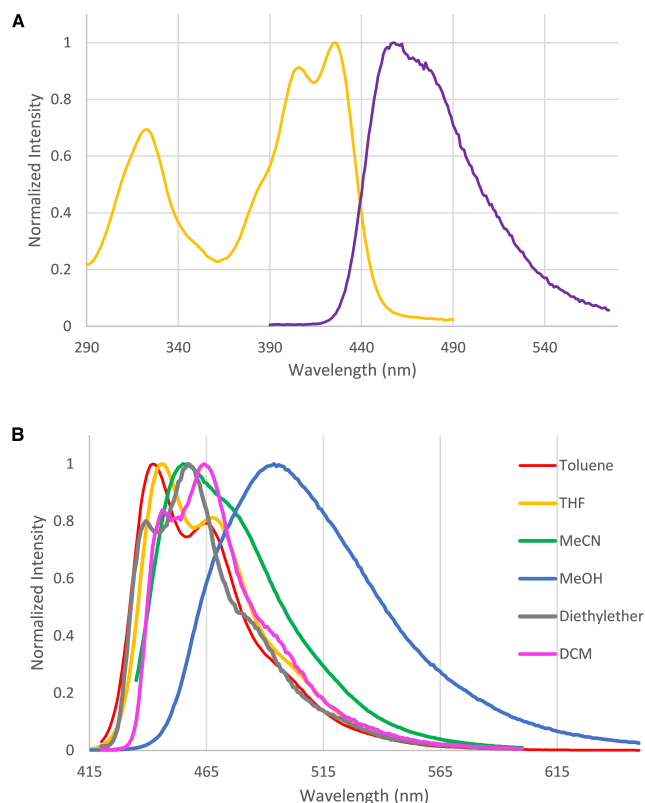


Figure 3. **A:** Absorption (yellow trace) and fluorescence emission (purple trace) of DNK **1**, 15 μM in acetonitrile. **B:** Fluorescence emission spectra of **1** collected in 6 solvents, 15 μM . See S.I. for data of DNK **3**.

Comprehensive and quantitative data was subsequently collected for the three model DNKs **1-3** along with two comparator compounds, PhBDAN **4** and the diamine fragment **5**. The data confirm that this new DNK scaffold presents unique fluorescence properties and markedly improved quantum yields over both comparators in both the solution (Table 1) and the solid state (Table 2). Comparing data for regioisomers **1** and **3**, it is evident that the intramolecular carbonyl---HN bond of **1** is not

essential, though both compounds differ slightly. DNK **1** has a notably smaller Stokes shift, whereas class member **3** exhibits extremely high fluorescence quantum yields of 89% and 85% in toluene and acetonitrile, respectively. Solvent studies performed on DNKs **1** and **3** (Figures 3B, S3) revealed positive solvatochromism in their emission bands, suggesting a change in dipole moment of the molecule in transition from ground to excited state. Considering the polarity index of acetonitrile is higher than methanol, the large solvatochromic effect with the latter may be due to its hydrogen bonding capacity, which may have a major impact on the FMOs owing to the contribution of the NH and carbonyl moieties. Comparators **4** and **5** show dramatically different optical profiles with very large Stokes shifts and broad, red-shifted emission bands (Table 1), demonstrating that both the boron and ketone moieties are key to the observed optical behaviour of DNKs.

It is also evident that the nature of the acyl group has a marked effect on the DNKs' fluorescence properties. Compared to **1**, the CF₃ group endows **2** with pronounced red shifts in both bands and greater solvatochromism between the two solvents, with a concomitant drop in the solution phase quantum yields. This may indicate that DNK **2** has an excited state with a larger dipole and which requires more geometric rearrangement. Non-radiative relaxation mechanisms, may become more efficient with a smaller HOMO-LUMO gap or the unique vibrational modes of the C-F moieties. DFT calculations of molecular orbitals were performed for PhBDAN (**4**) and DNKs **1-3**, and corroborate much of the above observations (Figure 4). Compared with PhBDAN (**4**) the electrostatic map of DNKs **1-3** shows reduced charge within the diaminophanthy unit with significant polarization towards the acyl units. Recent NICS calculations suggest the N-B-N ring of PhBDAN (**4**) is antiaromatic.¹¹ Like **4**, DNKs **1-3** show little density in the N-B-N ring. Remarkably, acylation causes an inversion of the relative energies of the LUMO and LUMO+1, along with a decrease of the absolute energy level. As a result, both HOMO and LUMO are localized onto the DNK unit, turning it into an independent chromophore, which supports the lack of influence of the nature of the B-aryl group observed with DNKs **1** and **S6-S8**.¹⁴ The FMOs of DNKs are significantly polarized, and the LUMO highlights the involvement of the B and N atoms. The HOMO-LUMO gaps of compounds **1-4** are consistent with their relative values of λ_{abs} , which suggests S₀→S₁ (π - π^*) transitions.

Table 1. Photophysical data for three DNKs 1-3 and two comparators 4-5 in solution.

com- pound	CH ₃ CN (15 μM)					toluene (15 μM)					
	λ _{abs} (nm)	λ _{em} (nm)	ε (M ⁻¹ cm ⁻¹)	Stokes shift (cm ⁻¹)	φ (%) ^[a]	λ _{abs} (nm)	λ _{em} (nm)	ε (M ⁻¹ cm ⁻¹)	Stokes shift (cm ⁻¹)	φ (%) ^[a]	Solvatochromic shift (cm ⁻¹) ^[b]
1	425	455	16400	1550	51	426	442	11550	850	37	646
2	449	540	12000	3750	4	454	507	11900	2300	9	1210
3	399	471	13500	3830	84	391	460	9530	3840	89	508
4	328	516	13600	11100	2	330	467	13000	8890	3	2030
5	377	538	11000	7930	8	371	540	7140	8440	16	-69

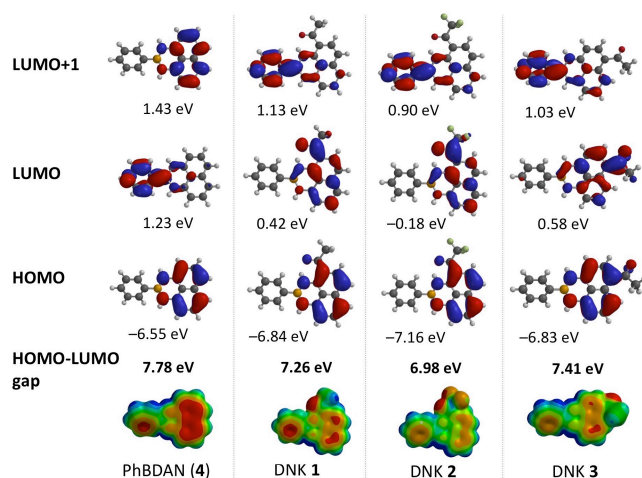
[a] Quantum yields were collected in nitrogen-degassed solvent and determined using an integrating sphere. [b] Solvatochromic shift was calculated as the difference in cm⁻¹ between the emission bands for toluene and acetonitrile.

Table 2. Solid state photophysical data for DNKs 1-2 and PhBDAN 4^[a]

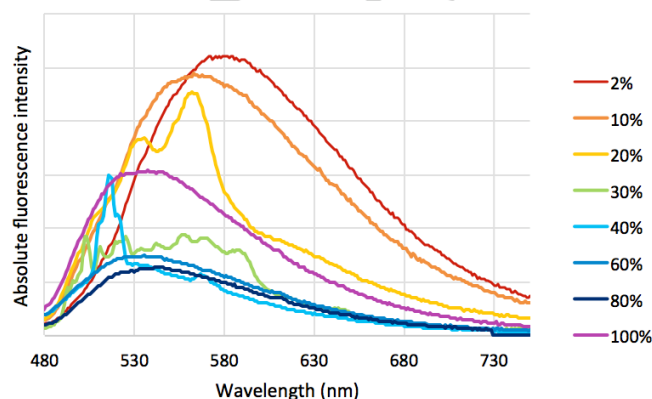
compound ^[a]	λ _{em} (nm)	φ (%)
1	550	8
2	525	7
4	462 ⁷	2.6 ⁷



[a] Solid state quantum yield measurements were performed on powdered solids in glass tubes under argon atmosphere, with barium sulfate as a scattering standard, and determined using an integrating sphere. Photograph in the rights shows DNK 1 under a hand-held UV lamp.

**Figure 4.** DFT calculations of PhBDAN (4) and DNKs 1-3 (ωB97X-D/6-31G*).

The solid state luminescence emission peaks for 1 and 2 were red shifted and broadened compared to the spectra in solution, presumably due to intermolecular π-π interactions (Table 2). Noting that the solution and solid quantum yields for DNK 2 are remarkably similar, it appeared this compound could provide a suitable platform for aggregation-induced emission (AIE).¹⁷ To investigate the fluorescence of aggregates in solution, water was chosen as the poor solvent and acetonitrile the good solvent. Solutions of equal concentration in 2 were prepared with varying proportions of water to acetonitrile and their absolute fluorescence intensity compared (Figure 5). The data confirm that DNK 2 exhibits AIE, and at superior quantum yields compared to the aryl-BDAN AIEgens reported recently.¹¹

**Figure 5.** Fluorescence emission of DNK 2 in organic-aqueous mixtures. Percentages indicate v/v percentage of acetonitrile to water. All solutions were measured at equal concentration of fluorophore (15 μM) and identical instrument settings, including excitation wavelength (450 nm).

However, unlike the classical behaviour expected of AIEgens,¹⁸ 2 displays a non-linear relationship between proportion of water and fluorescence intensity; although the 2% solution has the strongest fluorescence, fluorescence intensity is lowest around 80%, not 100%, acetonitrile. Furthermore, there appears to be fine structure to the emission bands for solvent systems of intermediate ratio (20-60%). The nature of the aggregate structure may qualitatively change along the solvent gradient. Although further study is required for more concrete interpretation of these unusual features, the existence of an AIE effect increases the relevance of this new DNK compound class to biological¹⁹ or solid state materials²⁰ applications, such as cellular imaging and organic light-emitting diodes. Further, the excitation wavelengths of DNKs (399-450 nm) are within range of those useful for near-infrared two-photon microscopy.

To exploit the remarkable properties of DNKs, a proof-of-concept was designed to address the need to detect residual boronic acid in active pharmaceutical ingredients. In recent years, evidence has emerged that suggests some boronic acids may be mutagenic and present a peril to human health.^{21,22} This finding is cause for caution in the pharmaceutical industry, as boronic acids are one of the most common synthetic intermediates:³ the Suzuki-Miyaura cross-coupling accounts for an impressive 12% of all reactions performed for drug discovery and development.²³ There is particular concern when the Suzuki-Miyaura reaction is employed late in a synthetic sequence, as low concentration (<10 ppm) boronic acids are difficult to detect by HPLC and NMR, but may still pose a health hazard.^{24,25} The straightforward mix-and-stir reaction conditions

of Scheme 1 suggested that the diamine **5** could form DNK adducts *in situ* with boronic acids and act as a fluorogenic chemosensor. The strong fluorescence of DNK **3**, along with the observation that phenyl ring substitution does not exert a significant influence on fluorescence in solution, indicate that this trace quantitation strategy could be both highly sensitive and robust to a wide variety of boronic acid intermediates.

To eliminate background noise from the intrinsic fluorescence of diamine **5**, HPLC analysis was chosen for peak separation and fluorescence detection. To this end, DNK **3** demonstrated good stability to a variety of HPLC conditions, including acidic eluent. Next, samples were prepared and reaction conditions were designed to model quantitation of trace boronic acid starting material in a pharmaceutical intermediate arising from a typical Suzuki-Miyaura reaction. Thus, a series of standards were prepared, each as a solid “cake” of trace phenylboronic acid in a matrix of biphenyl with a range of 1–20 ppm concentrations. To ensure quantitative conversion to DNK **3** in reasonable time, a large excess of diamine **5** in a concentrated solution were found to be essential. Acetonitrile was chosen as the solvent with gentle heating (Figure 6A).

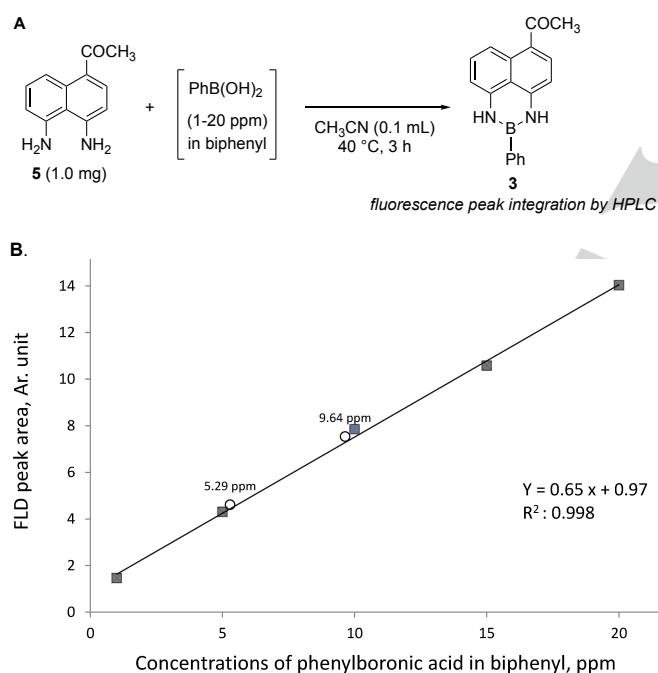


Figure 6. A. Reaction conditions used to detect boronic acid contaminant in unknown samples along with a set of standard samples. B. Calibration curve with different boronic acid concentration. Fluorescence peak areas were determined from HPLC chromatograms (λ_{ex} 410 nm, λ_{em} 485 nm). Plain squares: standards. Circles: test runs.

The integration of the fluorescent peak corresponding to DNK adduct **3** were determined by HPLC analysis for each standard. The resulting calibration curve (Figure 6B) was remarkably accurate ($R^2 \sim 0.99$) and linear down to the lowest 1 ppm standard. To validate the method and infer the trace quantity of phenylboronic acid in an unknown pharmaceutical sample, two test runs were validated to within 95% accuracy. Compared to other reagents,²⁵ diamine **5** provides much higher quantum yields and was demonstrated on a crude solid sample.

In summary, we have described the synthesis, structure, photophysical properties, and applications of a new luminescent polyaromatic boronic scaffold (diazaboryl-naphthyl-ketones, or DNKs). These compounds differ from BDAN **4** and benzodiazaboroles in that they are capable of extremely bright fluorescence, yet small structural modification unlocks dramatically and qualitatively different photophysical properties like aggregation-induced emission, positive solvatochromism, and solid state fluorescence. Photophysical data in solution and solid state revealed blue-shifted, narrowed, and intense emissions for DNKs **1–3** (up to 89% quantum yield) much superior to **4** and diamine **5**. DFT calculations of molecular orbitals revealed that unlike PhBDAN (**4**), the LUMO of **1–3** is localized onto the DNK unit, turning it into an independent chromophore, which supports the experimental observation that substitution on the B-phenyl group does not alter luminescence. The DNKs' advantageous properties were demonstrated with a preliminary analytical method for the low-ppm quantitation of trace boronic acid contaminants in pharmaceutical intermediates.

Acknowledgements

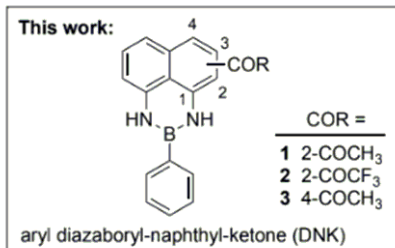
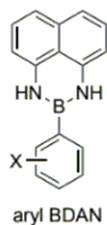
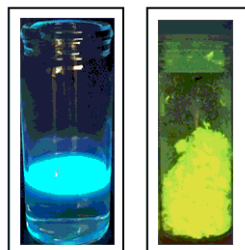
This work was funded by the Natural Sciences and Engineering Research Council (NSERC) of Canada (Discovery Grant to D.G.H.) and Alberta Innovates (Scholarship to HH). We thank Dr. Michael J. Ferguson and Dr. Yuqiao Zhou (X-ray Crystallography Laboratory, University of Alberta) for X-ray crystallographic analysis of compounds **1** and **2**, and, for advice and support with photophysical measurements: Prof. Rik Tykwinski, Prof. E. Rivard, Dr. Sarah Parke, and Wayne Moffatt.

Keywords: AIEgen • boronic acids • diazaborines • luminescence • trace analysis

- [1] X.-Y. Wang, X. Yao, A. Narita, K. Müllen, *Acc. Chem. Res.* **2019**, *52*, 2491–2505.
- [2] M. J. D. Bosdet, W. E. Piers, *Can. J. Chem.* **2009**, *87*, 8–29.
- [3] X.-Y. Wang, J.-Y. Wang, J. Pei, *Chem. Eur. J.* **2015**, *21*, 3528–3539.
- [4] X. Giustra, S.-Y. Liu, *J. Am. Chem. Soc.* **2018**, *140*, 1184–1194.
- [5] For a recent example: T. Kaehler, M. Bolte, H.-W. Lerner, M. Wagner, *Angew. Chem.* **2019**, *131*, 11501–11506; *Angew. Chem. Int. Ed.* **2019**, *58*, 11379–11384.
- [6] D. G. Hall, *Boronic Acids. Preparation and Applications in Organic Synthesis, Medicine and Materials*, 2nd Completely Revised ed.; Hall, D. G., Ed.; Wiley-VCH: Weinheim, Germany, **2011**.
- [7] H. Noguchi, K. Hojo, M. Suginoe, *J. Am. Chem. Soc.* **2007**, *129*, 758–759.
- [8] L. Weber, *Coord. Chem. Rev.* **2008**, *252*, 1–31.
- [9] L. Weber, L. Böhlring, *Coord. Chem. Rev.* **2015**, *284*, 236–275.
- [10] G. H. M. Davies, G. A. Molander, *J. Org. Chem.* **2016**, *81*, 3771–3779.
- [11] W.-M. Wan, D. Tian, Y.-N. Jing, X.-Y. Zhang, W. Wu, H. Ren, H.-L. Bao, *Angew. Chem.* **2018**, *130*, 15736–15742; *Angew. Chem. Int. Ed.* **2018**, *57*, 15510–15516.
- [12] T. Sugasawa, T. Toyoda, M. Adachi, K. Sasakura, *J. Am. Chem. Soc.* **1978**, *100*, 4842–4852.
- [13] AlCl₃ may form a chelate with both N atoms, thus preventing the normal boron-directed mechanism of the Sugasawa reaction to occur, allowing a Houben-Hoesch-like acylation to proceed in the para position.
- [14] See Supporting Information for additional details.

- [15] CCDC 1995194 (DNK 1) and 1995193 (DNK 2) contain the supplementary crystallographic data for this paper. It can be obtained free of charge from The Cambridge Crystallographic Data Centre.
- [16] C. A. Slabber, C. Grimmer, M. P. Akerman, R. S. Robinson, *Acta Crystallogr. Sect. E Struct. Rep. Online* **2011**, *67*, o1995–o1995.
- [17] Y. Hong, J. W. Y. Lam, B. Z. Tang, *Chem. Commun.* **2009**, 4332–4353.
- [18] Y. Chen, J. W. Y. Lam, R. T. K. Kwok, B. Liu, B. Z. Tang, *Mater. Horiz.* **2019**, *6*, 428–433.
- [19] C. Zhu, R. T. K. Kwok, J. W. Y. Lam, B. Z. Tang, *ACS Appl. Bio Mater.* **2018**, *1*, 1768–1786.
- [20] J. Mei, Y. Hong, J. W. Y. Lam, A. Qin, Y. Tang, B. Z. Tang, *Adv. Mater.* **2014**, *26*, 5429–5479.
- [21] M. M. Hansen, R. A. Jolly, R. J. Linder, *Org. Process Res. Dev.* **2015**, *19*, 1507–1516.
- [22] M. R. O'Donovan, C. D. Mee, S. Fenner, A. Teasdale, D. H. Phillips, *Mutat. Res. Toxicol. Environ. Mutagen.* **2011**, *724*, 1–6.
- [23] J. Boström, D. G. Brown, R. J. Young, G. M. Keserü, *Nat. Rev. Drug Discov.* **2018**, *17*, 709–727.
- [24] I. Patel, C. J. Venkatramani, A. Stumpf, L. Wigman, P. Yehl, *Org. Process Res. Dev.* **2017**, *21*, 182–186.
- [25] Y. Hattori, T. Ogaki, M. Ishimura, Y. Ohta, M. Kiriata, *Sensors* **2017**, *17*, 2436.

Entry for the Table of Contents



- simple, stable scaffold with quantum yields up to 89%
- positive solvatochromism & solid state luminescence
- boronic acid detection in crude mixtures down to 1 ppm

Do Not Know better. A small modification of the parent naphthodiazaborines affords stable diazaboryl-naphthyl-ketones (DNKs), unlocking new photophysical properties, including extremely bright fluorescence and aggregation induced emission, with promising applications in optoelectronics and chemical analysis such as the low-ppm quantitation of trace boronic acid contaminants in pharmaceutical intermediates.

Institute and/or researcher Twitter usernames: @HallBoronLab